ASME 434 Atmospheric Dynamics II
Department of Physics
Applied Science & Technology PhD Program
NC A&T State University (NCAT)

Prof. Yuh-Lang Lin
ylin@ncat.edu
http://mesolab.org

# Introduction to Mesoscale Instabilities

## Ch. 11 Mesoscale Instabilities

(Based on Ch. 7, "Mesoscale Dynamics", by Y.-L. Lin 2007)

### 11. Mesoscale Instabilities

7.1 Wave Energy Transfer through Instabilities
7.2 Integral Theorems of Stratified Flow
7.3 Static, Conditional, and Potential Instabilities
7.4 Kelvin-Helmholtz Instability
7.5 Inertial Instability
7.6 Symmetric Instability
7.7 Baroclinic Instability

[Chapter, equation and figure numbers of the lecture notes follow Lin (2007).]

## Chapter 7 Mesoscale Instabilities

- Observational, theoretical and numerical studies have found that instabilities play important roles in numerous mesoscale phenomena, such as

  Squall lines, rain bands, mesoscale convective complexes (MCC), mesoscale convective systems, mesoscale fronts, mesoscale cyclogenesis, clear air turbulence (CAT), billow clouds, heavy orographic precipitating systems, etc.

- Thus, a fundamental understanding of the instabilities occurring at mesoscale and those that influence mesoscale circulations is essential to comprehend these phenomena.

- For example, the momentum and/or potential energy associated with the airflow might be transferred into perturbation kinetic energy through instabilities, which may then disturb the flow or help release latent heating, dramatically disturbing the airflow.

- As discussed in Chapter 1 (Lin 2007), mesoscale instabilities may serve as one type of energy generation mechanism for mesoscale circulations and weather systems.

- Although instabilities associated with the mean wind velocity or thermal structure of the atmosphere are a rich energy source of atmospheric disturbances, the maximum growth rates of most atmospheric instabilities are either on the large scale, such as baroclinic and barotropic instabilities, or on the microscale, such as Kelvin-Helmholtz and static (gravitational) instabilities.

- Symmetric instability appears to cover the mesoscale range in the sense that the projected horizontal scale of the slantwise circulation of the unstable mode is often in the mesoscale range.

- Differences between moist and dry convection.

- In a dry atmosphere, convection includes both unstable updrafts and downdrafts and turbulent eddies, such as the boundary convection in the afternoon and Rayleigh-Bénard convection (Chandrasekar 1961) triggered by the thermal instability between two horizontal plates heated from below.

- Normally, moist convection in the atmosphere behaves quite differently from dry convection has and the mesoscale cellular convection shown in Fig. 7.1, and is characterized by (Emanuel and Raymond 1984):
  (1) Strong, compact, turbulent, unstable, upward motion,
  (2) Weak, compensated, laminar, stable downward motion (over a wide area of the surroundings), and
  (3) Gravity or inertia-gravity waves generated outside and which propagate away from the convective region.

- However, the differences described above may be due to the spatial distribution of the forcing.

- For example, Figure 7.1 show an example of a mesoscale cellular convection occurred over the Atlantic Ocean observed over the Atlantic Ocean off the southeast coast of the United States on February 19, 2002, as viewed by satellite Terra.

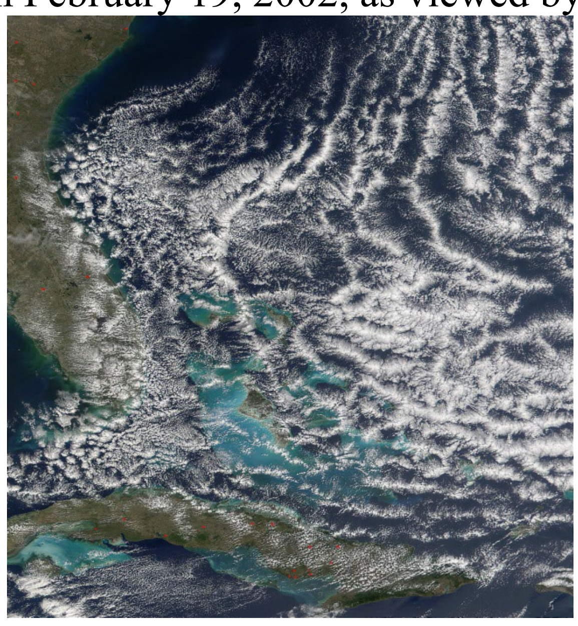

Fig. 7.1: Open cell cloud formation observed over the Atlantic Ocean off the southeast coast of the United States on February 19, 2002, as viewed by satellite Terra. This type of clouds is an atmospheric manifestation of Ralyleigh-Bénard convection is known as mesoscale cellular convection. It normally forms as the cold air passes over the warmer ocean waters. Notice the hexagonal open cells produced in the cloud-topped boundary layer and the convective clouds at the vertices of the hexagonal cells. (From Visible Earth, NASA) (Lin 2007)

- The open cells have downward motion and clear skies at the center of the cells. Notice the hexagonal open cells produced in the cloud-topped boundary layer and the convective clouds at the vertices of the hexagonal cells.
- This type of clouds is an atmospheric manifestation of Rayleigh-Bénard convection in the atmosphere. It normally forms as the cold air passes over the warmer ocean waters. Notice the hexagonal open cells produced in the cloud-topped boundary layer and the convective clouds at the vertices of the hexagonal cells.

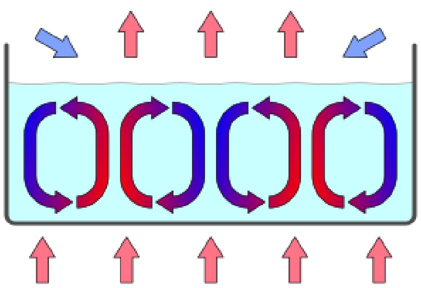

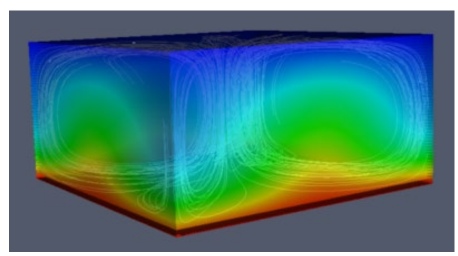

A sketch of 2D Rayleigh–Bénard convection in 2D Rayleigh–Bénard convection in 3D

(http://en.wikipedia.org/wiki/Rayleigh%E2%80%93B%C3%A9nard_convection)

Animation of 2D Rayleigh-Benard convection:1

Animation of 2D Rayleigh-Benard convection: 2

Benard cell convection on a dishpan

## 7.1 Wave Energy Transfer through Instabilities

- The energy transfer among different forms, such as potential energy and kinetic energy associated with the basic [mean potential energy, mean kinetic energy] or perturbed [perturbation (eddy) potential energy, perturbation (eddy) kinetic energy] flows, and through different hydrodynamic instabilities may be understood by examining the linear energy equation.

- The governing equations for a small-amplitude, inviscid, Boussinesq atmosphere on a planetary *f*-plane can be combined into a single equation for the vertical velocity, as derived in Chapters 2 & 3,

  With the Boussinesq approximation, the linearized perturbation equations, (2.2.14) – (2.2.18),

$$\frac{\partial u'}{\partial t}+U\frac{\partial u'}{\partial x}+V\frac{\partial u'}{\partial y}+U_z w'-fv'+\frac{1}{\overline{\rho}}\frac{\partial p'}{\partial x}=0\,, \qquad (2.2.14)$$

$$\frac{\partial v'}{\partial t}+U\frac{\partial v'}{\partial x}+V\frac{\partial v'}{\partial y}+V_z w'+fu'+\frac{1}{\overline{\rho}}\frac{\partial p'}{\partial y}=0\,, \qquad (2.2.15)$$

$$\frac{\partial w'}{\partial t}+U\frac{\partial w'}{\partial x}+V\frac{\partial w'}{\partial y}-g\frac{\theta'}{\overline{\theta}}+\frac{p'}{\overline{\rho}H}+\frac{1}{\overline{\rho}}\frac{\partial p'}{\partial z}=0\,, \qquad (2.2.16)$$

$$\frac{1}{c_s^2}\left(\frac{\partial p'}{\partial t}+U\frac{\partial p'}{\partial x}+V\frac{\partial p'}{\partial y}+\overline{\rho}f(Vu'-Uv')\right)-\frac{\overline{\rho}}{H}w'+\overline{\rho}\nabla\cdot\mathbf{V}'=\frac{\overline{\rho}}{c_p\overline{T}}q'\,, \qquad (2.2.17)$$

$$\left(\frac{\partial \theta'}{\partial t}+U\frac{\partial \theta'}{\partial x}+V\frac{\partial \theta'}{\partial y}\right)+\frac{f\overline{\theta}}{g}(V_z u'-U_z v')+\frac{N^2\overline{\theta}}{g}w'=\frac{\overline{\theta}}{c_p\overline{T}}q'\,. \qquad (2.2.18)$$

The above equations can be combined as the following equation [Eq. (3.2.1)]:

$$\frac{D}{Dt}\left\{\frac{D^2}{Dt^2}\nabla^2 w'+f^2 w'_{zz}-\left(U_{zz}\frac{D}{Dt}+fV_{zz}\right)w'_x-\left(V_{zz}\frac{D}{Dt}-fU_{zz}\right)w'_y+N^2\nabla_H^2 w'+2f\left(U_z w'_{yz}-V_z w'_{xz}\right)\right\}$$
$$+2fU_zV_z\left(w'_{xx}-w'_{yy}\right)+2f\left(V_z^2-U_z^2\right)w'_{xy}-2f^2\left(U_z w'_{xz}+V_z w'_{yz}\right)=\frac{g}{c_pT_o}\frac{D}{Dt}\nabla_H^2 q',$$

(7.1.1)

➢ As also mentioned in earlier chapters, this equation represents a mesoscale atmospheric system which may contain the following generation mechanisms of:

- Pure and inertia-gravity waves
- Static instability
- Conditional instability
- Potential (convective) instability
- Kelvin-Helmholtz instability
- Symmetric instability
- Inertial instability
- Baroclinic instability
- Wave-CISK (conditional instability of the second kind)

➢ Assuming $V=0$ and adding the meridionally sheared zonal flow ($U_y \neq 0$), Eq. (7.1.1) becomes

$$\left(\frac{\partial}{\partial t}+U\frac{\partial}{\partial x}\right)E+\rho_o u'w'U_z+\rho_o u'v'U_y-\left(\frac{\rho_o gf}{N^2\theta_o}\right)v'\theta'U_z+\nabla\cdot(p'v')=\left(\frac{\rho_o g^2}{c_p T_o N^2\theta_o}\right)\theta' q' \quad (7.1.2)$$

where

$$E=\frac{\rho_o}{2}\left[\left(u'^2+v'^2+w'^2\right)+\left(\frac{g}{N\theta_o}\right)^2\theta'^2\right], \quad (7.1.3)$$

is the total perturbation energy.

The total perturbation energy consists of perturbation kinetic energy and perturbation potential energy, which are represented by the first and second terms inside the square bracket, respectively.

➢ Taking the horizontal integration of Eq. (7.1.2) over a single wavelength for a periodic disturbance or from -∞ to +∞ for a localized disturbance in both *x* and *y* directions gives

$$\frac{\partial \overline{E}}{\partial t} = -\rho_o(\overline{uw})U_z - \rho_o(\overline{uv})U_y + \left(\frac{\rho_o g f}{N^2\theta_o}\right)(\overline{v\theta})U_z - \frac{\partial}{\partial z}(\overline{pw}) + \left(\frac{\rho_o g^2}{c_p T_o N^2 \theta_o}\right)(\overline{\theta\, q}) \qquad (7.1.4)$$

Integrating (7.1.4) from the surface ( $z = z_s$ ) to the top of the physical domain or a finite-area numerical model ( $z = z_T$ ) yields

$$\underset{(1)}{\frac{\partial E_T}{\partial t}} = \underset{(2)}{-\rho_o \int_{z_s}^{z_T} \overline{uw}\, U_z dz} \underset{(3)}{- \rho_o \int_{z_s}^{z_T} \overline{uv}\, U_y dz} + \underset{(4)}{\left(\frac{\rho_o g f}{N^2\theta_o}\right) \int_{z_s}^{z_T} \overline{v\theta}\, U_z dz}$$

$$\underset{(5)}{-\overline{pw}(z_T)} + \underset{(6)}{\overline{pw}(z_s)} + \underset{(7)}{\left(\frac{\rho_o g^2}{c_p T_o N^2 \theta_o}\right) \int_{z_s}^{z_T} \overline{\theta q}\, dz.} \qquad (7.1.5)$$

where $E_T$ is the domain-integrated total perturbation energy.

- Term 1: Total rate of change in the total perturbation energy in the system.

- Term 2: The vertical momentum flux transfer between the kinetic energy of the basic (mean) flow ($U_z$) and the perturbation wave energy ( $\overline{uw}$ ).

  - When shear instability occurs, the energy is transferred from the basic state shear flow ($U_z$) to the perturbation ( $\overline{uw}$ ).

    For a 2D, incompressible flow, one may define a perturbation streamfunction $\psi$ such that,

$$u = \frac{\partial \psi}{\partial z}; \quad w = -\frac{\partial \psi}{\partial x} \tag{7.1.6}$$

With this definition, $uwU_z$ can be written as

$$uwU_z = -\left[\frac{\partial \psi}{\partial x} / \frac{\partial \psi}{\partial z}\right]\left(\frac{\partial \psi}{\partial z}\right)^2 U_z = \left[\frac{\partial z}{\partial x}\right]_\psi \left(\frac{\partial \psi}{\partial z}\right)^2 U_z, \tag{7.1.7}$$

since $d\psi = (\partial \psi / \partial x)dx + (\partial \psi / \partial z)dz = 0$ on a constant streamline line $\psi$.

This in turn implies that when there exists shear instability (i.e. term 1 > 0) under the situation of $U_z > 0$, we have on average over the vertical plane

$$\left[\frac{\partial z}{\partial x}\right]_\psi < 0. \tag{7.1.8}$$

- Therefore, the growing wave in an adiabatic stably stratified flow must have a phase tilt in an opposite direction of the shear vector, i.e., an upshear phase tilt (Fig. 7.2). This also implies that the updraft has an upshear tilt since it is out of phase with the stream function by a factor of $\pi / 2$.

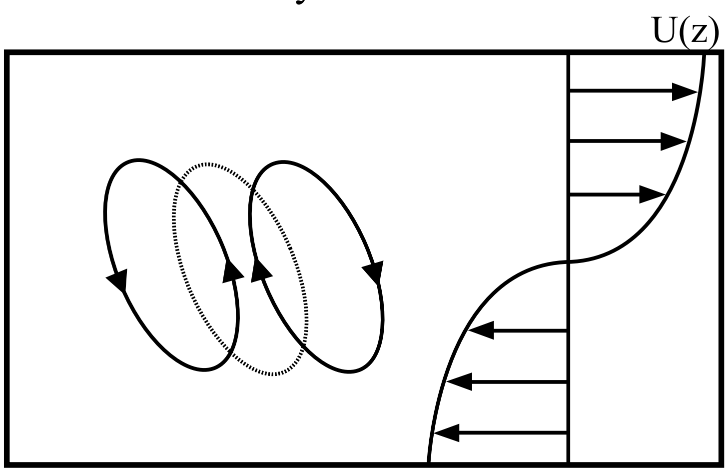


Fig. 7.2: A sketch of the basic wind profile and the upshear tilt of the perturbation streamfunctions (solid) and updraft (dashed) associated with an unstable growing gravity wave in

a stably stratified flow. The perturbation wave energy is converted from the basic flow shear. (From Lin and Chun, 1993) (Lin 2007)

(Animations: Ex. 1; Ex. 2; Reference: K-H instability)

Billow clouds often form along shear layers (separating air masses of differing moisture and temperature), and are thus subject to the Kelvin-Hlemholtz instability, particularly for sufficiently high shear velocities (photo credit: Brooks Martner, NOAA/ETL).

Billow clouds

Jupiter's *Great Red Spot* is a vortex tube (cat's eye) suistained by transonic shear layers in the planet's atmosphere. Note the smaller-amplitude K-H instabilities in the surrounding gas, as well as within the Red Spot itself (photo credit: NASA).

Jupiter’s Great Red Spot

- Term 3: When inertial instability occurs, the kinetic energy associated with the basic state shear ($U_y$) transfer to perturbation wave energy ($uv$).

  The argument for horizontal phase tilt is similar to the above argument for shear instability.

- Term 4: The energy exchange between the basic state vertical shear ($U_z$), which is supported by the baroclinicity (horizontal temperature gradient) through thermal wind balance, and the perturbation heat flux ($\overline{v\theta}$).

Under this situation, available potential energy is stored in the system, which is transferred to perturbation kinetic energy when baroclinic instability occurs.

This argument is used to explain why the trough tilts westward with height during the midlatitude cyclogenesis.

- Term 5: The forcing from the upper boundary condition.
- Term 6: The forcing from the lower boundary.
- Term 7: The contribution from diabatic source or sink to total perturbation energy.

**[Section 7.2 is for Reading Assignment]**

## 7.2 Integral Theorems of Stratified Flow

### *7.2.1 Governing equations*

Consider the following inviscid, nonrotating, Boussinesq fluid system with all the nonlinear and inhomogeneous terms lumped into source terms on the right side of the governing equations,

$$\frac{\partial u'}{\partial t} + U\frac{\partial u'}{\partial x} + U_z w' + \frac{1}{\rho_o}\frac{\partial p'}{\partial x} = F_1\,, \tag{7.2.1}$$

$$\frac{\partial v'}{\partial t} + U\frac{\partial v'}{\partial x} + \frac{1}{\rho_o}\frac{\partial p'}{\partial y} = F_2\,, \tag{7.2.2}$$

$$\frac{\partial w'}{\partial t} + U\frac{\partial w'}{\partial x} - g\frac{\theta'}{\theta_o} + \frac{1}{\rho_o}\frac{\partial p'}{\partial z} = F_3\,, \tag{7.2.3}$$

$$\frac{\partial u'}{\partial x} + \frac{\partial v'}{\partial y} + \frac{\partial w'}{\partial z} = 0\,, \tag{7.2.4}$$

$$\frac{\partial \theta'}{\partial t} + U\frac{\partial \theta'}{\partial x} + \frac{N^2\theta_o}{g}w' = H\,, \tag{7.2.5}$$

where

$$F_1 = -\frac{\partial(u'u')}{\partial x} - \frac{\partial(u'v')}{\partial y} - \frac{\partial(u'w')}{\partial z}\,, \tag{7.2.6}$$

$$F_2 = -\frac{\partial(v'u')}{\partial x} - \frac{\partial(v'v')}{\partial y} - \frac{\partial(v'w')}{\partial z}\,, \tag{7.2.7}$$

$$F_3 = -\frac{\partial(w'u')}{\partial x} - \frac{\partial(w'v')}{\partial y} - \frac{\partial(w'w')}{\partial z}\,, \tag{7.2.8}$$

$$H = \dot{Q} - \frac{g}{\theta_o}\left[\frac{\partial(u'\theta')}{\partial x} + \frac{\partial(v'\theta')}{\partial y} + \frac{\partial(w'\theta')}{\partial z}\right]. \tag{7.2.9}$$

| | |
|---|---|
| $F = (F_1, F_2, F_3)$ | perturbation *Reynolds stress*, |
| $\dot{Q}$ | diabatic heating, and |
| $H$ | *effective heating*, which is composed by the diabatic heating and *turbulent heat fluxes*. |

- Considering a 2D flow and taking the normal mode approach by assuming

$$\phi = \hat{\phi}\, e^{ik(x-ct)}\,. \tag{7.2.10}$$

Substituting it into (7.2.1) - (7.2.5) yields

$$\frac{\partial^2 \hat{w}}{\partial z^2} + m^2\hat{w} = \frac{\hat{H}}{(c-U)^2} + \left(\frac{1}{c-U}\right)\left(\hat{F}_{1z} - ik\hat{F}_3\right), \tag{7.2.11}$$

where

$$m^2 = \frac{1}{c-U}\frac{d^2U}{dz^2} + \frac{N^2}{(c-U)^2} - k^2\,. \tag{7.2.12}$$

Defining a new variable $h$ as

$$h \equiv \frac{\hat{w}}{c-U}, \tag{7.2.13}$$

It can be derived from (7.2.11),

$$\frac{\partial}{\partial z}\left[(c-U)^2\frac{\partial h}{\partial z}\right]+\left[N^2-k^2(c-U)^2\right]\,h=\frac{g}{\theta_o}\frac{\hat{H}}{c-U}+\hat{F}_{1z}-ik\hat{F}_3. \tag{7.2.14}$$

Taking $\mathrm{Im}\int_0^\infty h^*\cdot(7.2.14)dz$ yields

$$\mathrm{Im}\int_0^\infty h^*\frac{\partial}{\partial z}\left[(c-U)^2\frac{\partial h}{\partial z}\right]\,dz-\mathrm{Im}\int_0^\infty k^2(c-U)^2|h|^2\,\,dz$$

$$=\frac{g}{\theta_o}\mathrm{Im}\int_0^\infty\frac{\hat{w}^*\hat{H}}{|c-U|^2}\,dz+\mathrm{Im}\int_0^\infty h^*(\hat{F}_{1z}-ik\hat{F}_3)\,dz\,, \tag{7.2.15}$$

where $h^*$ is the complex conjugate of $h$, which is assumed to be 0 at $z$=0, ∞. Note that the term involving $N^2$ does not appear in (7.2.15) because it has no imaginary part. Substituting $c=c_r+ic_i$ into (7.2.15) and taking the imaginary part yields

$$-2\int_0^\infty c_i(c_r-U)\left[\left|\frac{\partial h}{\partial z}\right|^2+k^2|h|^2\right]dz=\mathrm{Im}\int_0^\infty\frac{\hat{w}^*\hat{H}}{|c-U|^2}dz+\mathrm{Im}\int_0^\infty h^*\left(\hat{F}_{1z}-ik\hat{F}_3\right)dz\,. \tag{7.2.16}$$

## Case (i): No forcing

Eq. (7.2.16) is reduced to

$$-2\int_0^\infty c_i(c_r-U)\left[\left|\frac{\partial h}{\partial z}\right|^2+k^2|h|^2\right]dz=0\,. \tag{7.2.17}$$

In order for instability to occur, $c_i$ must be greater than 0.

This implies that term $(c_r - U)$ must change sign somewhere between $z = 0$ and $\infty$ because the term in the square bracket is always positive. Therefore, ***there exists a critical level at which*** $U = c_r$ ***in order for instability to occur in a two-dimensional, nonrotating flow***.

**[For reference]**
**Case (ii)**: with only thermal forcing, Eq. (7.2.16) reduces to

$$-2\int_0^\infty c_i(c_r - U)\left[\left|\frac{\partial h}{\partial z}\right|^2 + k^2|h|^2\right]dz = \mathrm{Im}\int_0^\infty \frac{\hat{w}^*\hat{H}}{|c-U|^2}dz. \qquad (7.2.18)$$

Assume

$$H = Qe^{i\theta}w. \qquad (7.2.19)$$

After substituting Eq. (7.2.19) into Eq. (7.2.18), the right hand side of Eq. (7.2.18) becomes

$$\mathrm{Im}\int_0^\infty \frac{\hat{w}^*\hat{H}}{|c-U|^2}dz = \int_0^\infty \frac{Q|\hat{w}|^2\sin\theta}{|c-U|^2}dz \qquad (7.2.20)$$

If the heating is in phase with vertical velocity everywhere, i.e. $\theta = 0$, then

$$-2\int_0^\infty c_i(c_r - U)\left[\left|\frac{\partial h}{\partial z}\right|^2 + k^2|h|^2\right]dz = \mathrm{Im}\int_0^\infty \frac{\hat{w}^*\hat{H}}{|c-U|^2}dz = 0$$

This implies that either $c_i = 0$, where there is no amplification or instability, or $c_r = U$ at certain level, where a *steering* or *critical level* exists. This leads us to ***Bolton's theorem***: If a diabatic forcing is to generate an amplifying, non-steering level perturbation, the forcing must be somewhat out of phase with the vertical velocity (Bolton, 1980a; Moncrieff 1978).

### *7.2.2 Miles' Theorem*

For a two-dimensional, nonrotating, stratified shear flow with no forcing, Eq. (7.2.14) becomes

$$\frac{\partial}{\partial z}\left[(U-c)^2\frac{\partial h}{\partial z}\right] + \left[N^2 - k^2(U-c)^2\right]h = 0, \qquad (7.2.21)$$

with $h(z_1) = h(z_2) = 0$ as boundary conditions. Note that $h = \hat{w}/(c-U)$.

If the flow is unstable, then $c$ will be complex and $U-c\neq 0$ for any height $z$.

Letting $h=G/\sqrt{U-c}$ and substituting it into the above equation gives

$$c_i\left(\int_{z_1}^{z_2}\left[\left|\frac{\partial G}{\partial z}\right|^2+k^2|G|^2\right]dz+\int_{z_1}^{z_2}\left|\frac{G}{U-c}\right|^2\left(N^2-\frac{1}{4}U_z^2\right)dz\right)=0\,. \qquad (7.2.24)$$

Since the flow is unstable, it requires that $c_i>0$. [Remember we assume that $\phi=\hat{\phi}\,e^{ik(x-ct)}$ in (7.2.10).]

The above equation therefore implies that $Ri<1/4$ at some level between $z_1$ and $z_2$, where $Ri\equiv N^2/U_z^2$ is the *Richardson number*.

Thus, for instability to occur, it is necessary that $Ri<1/4$ somewhere in the fluid. On the other hand, *if* $Ri\geq 1/4$ *everywhere in the fluid system, then the fluid system is stable.* This is referred to as *Miles' Theorem*.

### *7.2.3 Howard's Semicircle Theorem*

Consider Eq. (7.2.11) with no forcing,

$$\frac{\partial^2\hat{w}}{\partial z^2}+m^2\hat{w}=0\,, \qquad (7.2.25)$$

where

$$m^2=-\frac{1}{U-c}\frac{d^2U}{dz^2}+\frac{N^2}{(U-c)^2}-k^2\,, \qquad (7.2.26)$$

Using the vertical displacement $\eta$ and substituting its relationship with $w$,

$$\hat{\eta}=\frac{\hat{w}}{ik(U-c)} \qquad (7.2.27)$$

into Eq. (7.2.25) yields

$$\frac{\partial}{\partial z}\left[(U-c)^2\frac{\partial\hat{\eta}}{\partial z}\right]+\left[N^2-k^2(U-c)^2\right]\hat{\eta}=0\,\cdot \qquad (7.2.28)$$

The boundary conditions are $\hat{\eta}=0$ at $z=z_1$ and $z_2$.

Multiplying Eq. (7.2.28) by the conjugate of $\hat{\eta}$ (i.e. $\hat{\eta}^*$) and then integrating from $z_1$ to $z_2$ leads to

$$\int_{z_1}^{z_2} (U-c)^2 \left( \left| \frac{\partial \hat{\eta}}{\partial z} \right|^2 + k^2 |\hat{\eta}|^2 \right) \mathrm{dz} \; - \int_{z_1}^{z_2} N^2 |\hat{\eta}|^2 dz = 0 \,. \tag{7.2.29}$$

Substituting $c = c_r + ic_i$ into the above equation and then separating the real and imaginary parts yields

$$\text{Real Part} = \int_{z_1}^{z_2} \left[ (U-c_r)^2 - c_i^2 \right] R \,\mathrm{dz} \; - \int_{z_1}^{z_2} N^2 |\hat{\eta}|^2 dz = 0 \tag{7.2.30}$$

$$\text{Imaginary Part} = 2c_i \int_{z_1}^{z_2} (U-c_r)\, R \;\mathrm{dz} \;= 0 \tag{7.2.31}$$

where

$$R = \left| \frac{\partial \hat{\eta}}{\partial z} \right|^2 + k^2 |\hat{\eta}|^2 \,. \tag{7.2.32}$$

Again, for instability to occur, we require $c_i > 0$. In turn, with (7.2.32), Eq. (7.2.31) requires that

$$\int URdz = c_r \int Rdz \,. \tag{7.2.33}$$

Equations (7.2.30) and (7.2.33) imply that

$$\int U^2 Rdz = \left( c_r^2 + c_i^2 \right) \int Rdz + \int N^2 |\hat{\eta}|^2 dz \,. \tag{7.2.34}$$

Now supposing $a \le U(z) \le b$, we then have

$$\left\{ \left[ c_r - (a+b)/2 \right]^2 + c_i^2 - \left[ (a-b)/2 \right]^2 \right\} \int Rdz + \int N^2 |\hat{\eta}|^2 dz \le 0 \,. \tag{7.2.35}$$

Since the last term on the left side of the above equation and the integration of $R$ with respect to $z$ are both positive, we require that

$$\left[ c_r - (a+b)/2 \right]^2 + c_i^2 \le \left[ (a-b)/2 \right]^2 \,. \tag{7.2.36}$$

This leads us to the *Howard semicircle theorem*: *The complex phase speed, c, of an unstable normal mode must lie within the semicircle enclosed by Umin (i.e. a) and Umax (i.e. b).* The Howard semicircle theorem can also be sketched as shown in Fig. 7.3.

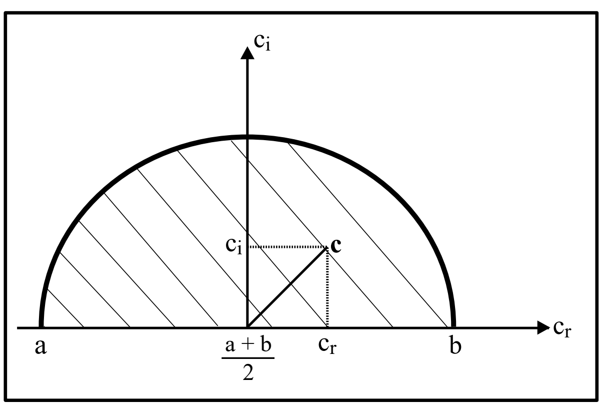


Fig. 7.3: A sketch of the Howard's semicircle theorem.

## 7.3 Static, Conditional, and Convective Instabilities

### *7.3.1 Static Instability*

- *Static instability* is also referred to in the literature as *buoyant instability* and *gravitational instability*, and describes an atmospheric state in which an air parcel will accelerate away from its original level due to the density difference between itself and its environment.

- It can be derived that (see Lin 2007, Holton 2004)

$$N^2 = \frac{g}{\bar{\theta}}\frac{\partial \bar{\theta}}{\partial z} = \frac{g}{T}(\Gamma_d - \gamma), \tag{7.3.5}$$

where

$N$ : *Brunt-Vaisala (buoyancy) frequency*,

$\gamma \equiv -\partial T/\partial z$ : observed *environmental (actual) lapse rate*

$\Gamma_d = g/c_p$ : *dry lapse rate.*

The overbar represents values of the environmental air.

The stability criteria for the displacement of a dry or unsaturated air parcel are

$$\begin{aligned} &\gamma < \Gamma_d : \textit{absolutely stable}, \\ &\gamma = \Gamma_d : \textit{dry neutral}, \\ &\gamma > \Gamma_d : \textit{dry absolutely unstable}. \end{aligned} \tag{7.3.6}$$

The vertical motion of the air parcel follows

$$\frac{Dw}{Dt} = \frac{D^2 \delta z}{Dt^2} = -\frac{1}{\rho}\frac{\partial p}{\partial z} - g, \tag{7.3.1}$$

where $\rho$ and $p$ are the density and pressure of the air parcel, respectively.

According to parcel theory, the pressure of the air parcel adjusts immediately to the pressure of its environment ($\bar{p}$), i.e. $p = \bar{p}$, which leads to

$$\frac{Dw}{Dt} = \frac{D^2 \delta z}{Dt^2} = g\left(\frac{\bar{\rho} - \rho}{\rho}\right) \equiv b, \qquad (7.3.2)$$

where $b$ is the *buoyancy* or the buoyancy force per unit mass, and the overbar denotes the environmental value. In deriving the above equation, we have assumed the environmental atmosphere is in hydrostatic balance.

Thus, (7.3.2) indicates that the vertical acceleration of the air parcel is controlled by the ***buoyancy force***, $g[(\bar{\rho} - \rho)/\rho]$. It can be derived that the buoyancy force (the right hand side of (7.3.2)), is approximately equal to $g[(\theta - \bar{\theta})/\bar{\theta}]$. At $z = 0$, the air parcel is assumed to have the same potential temperature ($\theta$) as that of its environment ($\bar{\theta}$).

It can be derived

$$\frac{D^2 \delta z}{Dt^2} + \mathrm{N}^2 \delta z = 0. \qquad (7.3.4)$$

The Brunt-Vaisala frequency measures the static stability of the air parcel's environment and is related to the change of the air parcel's buoyancy in relation to height,

$$N^2 = -\frac{\partial b}{\partial z} = \frac{g}{\bar{\theta}} \frac{\partial \bar{\theta}}{\partial z}. \qquad (7.3.5)$$

It can be easily proven that the criteria for static stability, static neutrality, and static instability are: $N^2 > 0$, $N^2 = 0$, and $N^2 < 0$, respectively.

The static instability acts on a horizontal scale of tens to thousands of meters. Static and shear instability produce most of the small-scale turbulence in the troposphere.

The stability criteria for dry air may also be determined by the vertical gradient of the environmental potential temperature:

$$N^2 > 0,\ \gamma < \Gamma_d, \text{ or } \partial\overline{\theta}/\partial z > 0: \textit{ absolutely stable},$$
$$N^2 = 0,\ \gamma = \Gamma_d, \text{ or } \partial\overline{\theta}/\partial z = 0: \textit{ dry neutral},$$
$$N^2 < 0,\ \gamma > \Gamma_d, \text{ or } \partial\overline{\theta}/\partial z < 0: \textit{ dry absolutely unstable}. \quad (7.3.6)$$

In the above criteria, $\partial\overline{\theta}/\partial z$ can be replaced by the dry Brunt-Vaisala frequency (*N*). The dry absolute instability is also referred to as *dry gravitational instability* in the literature.

- The vertical acceleration is contributed by the dynamic pressure ($p_d'$) and buoyancy pressure ($p_b'$). The dynamical pressure arises from the flow field differences created by the disturbance, and buoyancy pressure is generated by the vertical buoyancy gradient.

- Taking these effects into consideration, the vertical momentum equation can be written as

$$\frac{Dw}{Dt} = -\frac{1}{\rho_o}\frac{\partial p_d'}{\partial z} + \left(b - \frac{1}{\rho_o}\frac{\partial p_b'}{\partial z}\right), \quad (7.3.8)$$

$$-\frac{1}{\rho_o}\nabla^2 p_d' = |D|^2 - |\omega|^2, \quad (7.3.9)$$

$$-\frac{1}{\rho_o}\nabla^2 p_b' = -\frac{\partial b}{\partial z}. \quad (7.3.10)$$

where

$|D|$: total deformation and

$\boldsymbol{\omega}$: 3D vorticity vector.

$$|\boldsymbol{\omega}|^2 = (w_y - v_z)^2 + (u_z - w_x)^2 + (v_x - u_y)^2$$

$$|D|^2 = (u_x^2 + u_y^2 + u_z^2) + (v_x^2 + v_y^2 + v_z^2) + \{(w_x^2 + w_y^2 + w_z^2) - (d \ln \bar{\rho} / dz)\mathbf{v} \cdot \nabla w - (d^2 \ln \bar{\rho} / dz^2) w^2\}$$

- The first term on the right side of (7.3.10) is due to the dynamic perturbation pressure, which is independent of the thermodynamic base state.

- The buoyancy should include both terms inside the bracket on the right side of (7.3.10) (Doswell and Markowski 2004).

- It has been proposed and observed in the real atmosphere that ***moist absolute instability*** may be created and maintained as mesoscale convective systems develop (Bryan and Fritsch 2000).

- A strong, mesoscale, nonbuoyancy-driven ascent, such as mechanical lifting along surface-based outflow layers, frontal zones, or an elevated terrain, may bring a conditionally unstable environmental layer to saturation faster than small-scale, buoyancy-driven convective elements are able to overcome the unstable state.

- In addition, the lifting of a *moist absolutely unstable layer (MAUL)* tends to warm the environment, causing a reduction in the temperature difference between the environment and vertically displaced parcels, and thereby decreasing the buoyancy of convective parcels and helping to maintain the MAUL (Bryan and Fritsch 2000).

➢ Figure 7.4 illustrates how, in an idealized convective system, a MAUL forms ahead of a density current created through slab convective overturning.

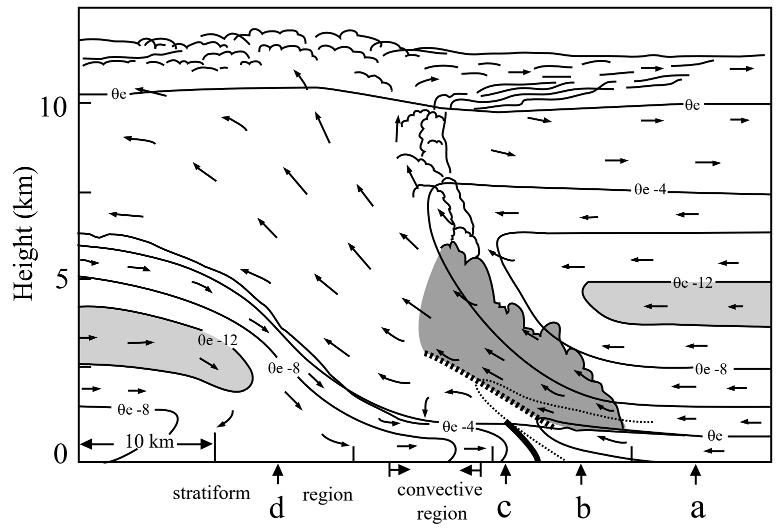


Fig. 7.4: A schematic of the formation of a MAUL through slab convective overturning. Wind vectors relative to the outflow boundary are denoted by arrows, cloud boundaries are denoted by scalloped lines, $\theta_e$ contours (every 4 K) are denoted by solid lines, the outflow boundary or frontal zone is denoted by heavy solid line, midlevel layer of low $\theta_e$ is highlighted by light shading, and the MAUL is depicted by dark shading. (From Bryan and Fritsch 2000)

### *7.3.2 Conditional Instability*

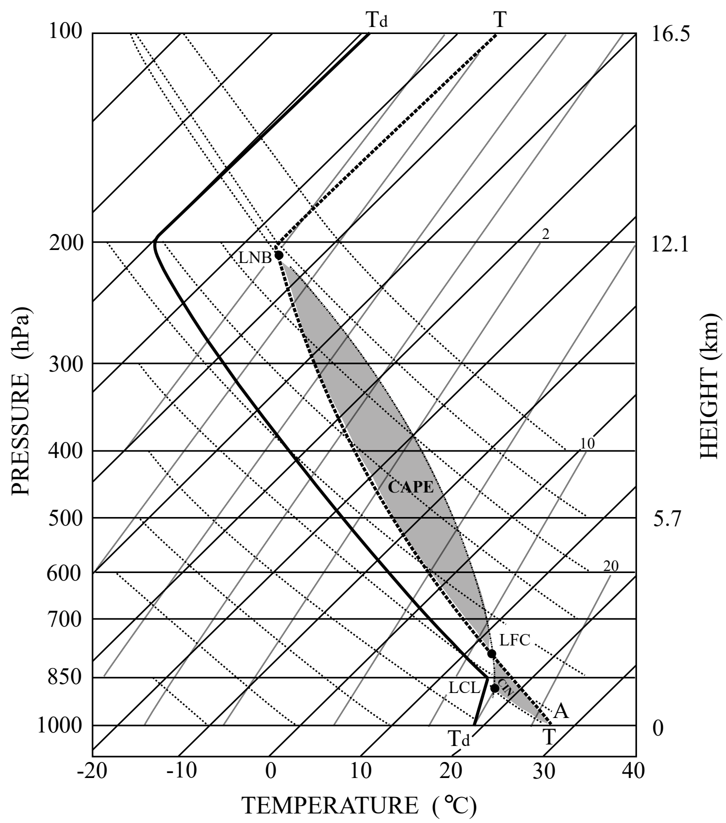


Fig. 7.5: Example of a sounding with conditional instability displayed on a *skew-T log-p* thermodynamic diagram. The lifting condensation level (LCL), level of free convection (LFC), and level of neutral buoyancy (LNB) for the air parcel originated at A are denoted in the figure. The convective available potential energy (CAPE) is the area enclosed by the temperature curve (thick dashed line) and moist adiabat (dot-dashed curve) in between LFC and LNB, while the convective inhibition is the area enclosed the temperature curve and dry adiabat (below LCL) and moist adiabat (above LCL) in between the surface and the LFC.

*Lifting condensation level* (*LCL*)
*Level of free convection* (*LFC*).
*Level of neutral buoyancy (LNB)*
*Convective available potential energy* (*CAPE*):

$$CAPE = \int_{z_{LFC}}^{z_{LNB}} B\,dz = \int_{z_{LFC}}^{z_{LNB}} g\left(\frac{\bar{\rho}-\rho}{\rho}\right)dz = \int_{z_{LFC}}^{z_{LNB}} g\left(\frac{T-\bar{T}}{\bar{T}}\right)dz = \int_{z_{LFC}}^{z_{LNB}} g\left(\frac{\theta-\bar{\theta}}{\bar{\theta}}\right)dz\,. \quad (7.3.17)$$

The *moist adiabatic lapse rate*

$$\Gamma_s \equiv -\frac{dT}{dz} = \frac{\Gamma_d}{1+(L/c_p)(dq_{vs}/dT)}, \quad (7.3.18)$$

where $\Gamma_d$ is the dry adiabatic lapse rate,

$L$ is the latent heat of condensation or sublimation, and

$q_{vs}$ is the saturation water vapor mixing ratio.

CIN: The negative area represents the energy needed to lift an air parcel to its *LFC* and is also known as the *convective inhibition CIN*. Mathematically, *CIN* may be defined as

$$CIN = -\int_{z_i}^{z_{LFC}} g\left(\frac{T-\bar{T}}{\bar{T}}\right)dz\,. \quad (7.3.22)$$

Thus, the *CIN* is the energy required to lift an air parcel vertically and pseudoadiabatically to its level of free convection.

The maximum updraft can may be estimated by

$$w_{\max} = \sqrt{2CAPE}\,.$$

When rain evaporates in sub-saturated air or solid precipitate (snow or hail) melts at the melting level, a downdraft will be generated by the cooled air. The maximum downdraft may be estimated as $-w_{\max} = \sqrt{2DCAPE_i}$, where $DCAPE_i$ is the *downdraft convective available potential energy* and is defined as

$$DCAPE_i = -\int_{z_i}^{z_s} g\left(\frac{T-\overline{T}}{\overline{T}}\right)dz\,, \qquad (7.3.23)$$

where $z_s$ is normally the surface or the level at which an air parcel descends from the original level $z_i$, allowing a neutral buoyancy to be achieved. Cooling the parcel to saturation via the wet-bulb process and then descending it saturated- or pseudo-adiabatically, leaving enough evaporation to keep the air parcel saturated will allow one to obtain the parcel temperature (e.g. Emanuel 1994).

- The criterion for conditional instability may also be determined via the vertical gradient of the *saturation equivalent potential temperature* ($\theta_e^*$), which is defined as the equivalent potential temperature of a hypothetically saturated atmosphere. This hypothetical atmosphere has the same thermal structure as the actual atmosphere.

- In other words, the $\theta_e^*$ can be defined as the equivalent potential temperature the air parcel would have if it were saturated at the same pressure and temperature,

$$\theta_e^* = \theta \exp(Lq_{vs} / c_p T)\,. \qquad (7.3.24)$$

- It can be derived

$$\frac{D^2\delta z}{Dt^2} + \left(\frac{g}{\overline{\theta}_e^*}\frac{\partial \overline{\theta}_e^*}{\partial z}\right)\delta z = 0$$

Therefore, the conditional stability criterion for a saturated layer of air becomes

$$\frac{\partial \overline{\theta}_e^*}{\partial z} \begin{cases} > 0 & \text{conditionally stable} \\ = 0 & \text{conditionally neutral} \\ < 0 & \text{conditionally unstable} \end{cases} \tag{7.3.29}$$

Based on the above discussion, there exist six static stability states for dry and moist air:

1) absolutely stable $\gamma < \Gamma_s$ ,
2) saturated neutral $\gamma = \Gamma_s$ ,
3) conditionally unstable $\Gamma_s < \gamma < \Gamma_d$ , (7.3.30)
4) dry neutral $\gamma = \Gamma_d$ ,
5) dry absolute unstable $\gamma > \Gamma_d$ ,
6) moist absolutely unstable $\gamma_s > \Gamma_s$ .

### *7.3.3 Potential Instability*

- *Potential instability* is also referred to as *convective instability* in the literature, and describes a condition in which an atmospheric layer becomes unstable statically after lifting.
- It is based on layer theory.

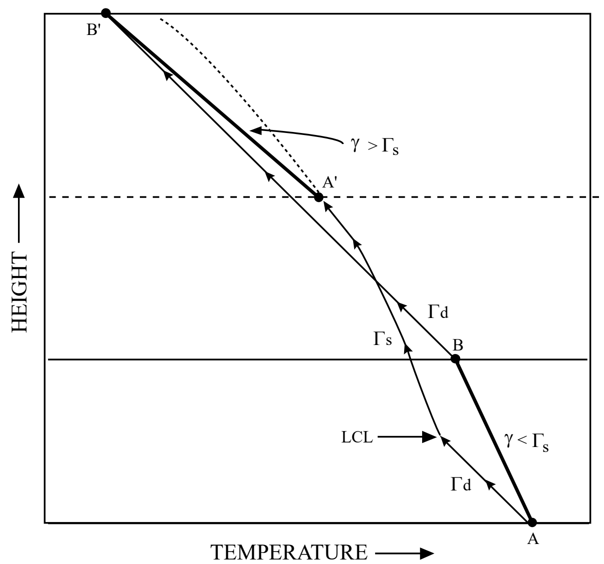


Fig. 7.6: Illustration of potential (convective) instability by lifting an initially absolute stable layer AB with $\partial\overline{\theta}_e/\partial z < 0$. The top of the layer (B) follows a dry adiabat to saturation at B', while the bottom of the layer becomes saturated earlier and then follows moist adiabat to A'. The lapse rate of the final saturated layer (A'B') is greater than the moist adiabat, thus is unstable. (Adapted after Darkow 1986)

- The criteria for potential (convective) instability may be expressed in terms of the equivalent potential temperature.

$$\frac{\partial\overline{\theta}_e}{\partial z}\begin{cases} > 0 & \text{potentially stable} \\ = 0 & \text{potentially neutral} \\ < 0 & \text{potentially unstable} \end{cases} \qquad (7.3.31)$$

Example of Potential (Convective) Instability from soundings:
Miller Type I "loaded gun sounding":



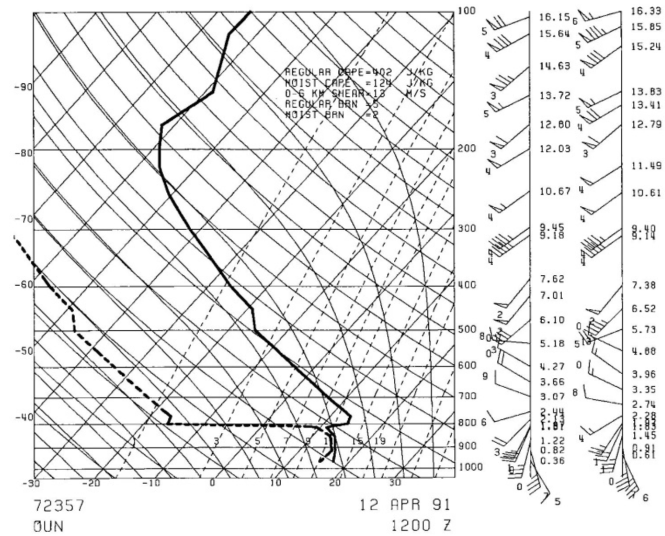


**Figure 3.10** Example of a typical Miller "Type I" sounding in the United States. Sounding is at Norman, Oklahoma, at 1200 UTC, April 12, 1991 (0600 LST). Skewed abscissa and logarithmic ordinate are temperature (°C) and pressure (mb), respectively. The plot of temperature and dew point are given by the thick solid and dashed lines, respectively. Winds plotted at the right; pennant = 25 m s$^{-1}$; whole barb = 5 m s$^{-1}$; half barb = 2.5 m s$^{-1}$. The moist air in the boundary layer (surface to 810 mb) comes from the Gulf of Mexico; the mixing ratio from the surface to 850 mb is nearly constant. The layer of low static stability above the moist layer comes from an elevated, deep, dry boundary layer over Mexico. The air above the Mexican layer (above 450 mb) comes from the western United States. The latter is separated from the former by a 50-mb deep stable layer. A stable layer, which in this case is an inversion, caps the moist layer around 800 mb. Several tornadic thunderstorms occurred in north-central Oklahoma later on in the day.

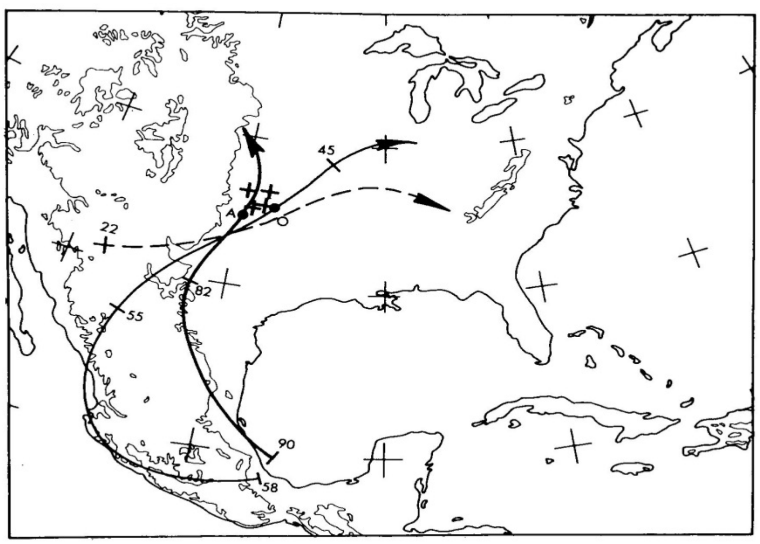

**Figure 3.11.** Illustration of air trajectories that produce Miller "Type I" soundings in the United States. Composite chart for May 4, 1961. Limiting trajectories for the moist, trade-wind flow (thick line; height of top of layer indicated in tens of mb) and the top of the Mexican air (thin line; height marked in tens of mb). Flow in the high troposphere, at about 220 mb (dashed line). Altus (A) and Oklahoma City (O) denoted by full circles (from Carlson and Ludlam, 1963; courtesy Toby Carlson).

# Miller Type I "loaded gun sounding"

Loaded gun sounding provides an environment conducive to "potential (convective) instability", instead of "conditional instability", thus nothing to do with CAPE!

However, if a sounding satisfies both PI and CI (large CAPE+forcing to lift to LFC), then the convection being triggered could be very severe!

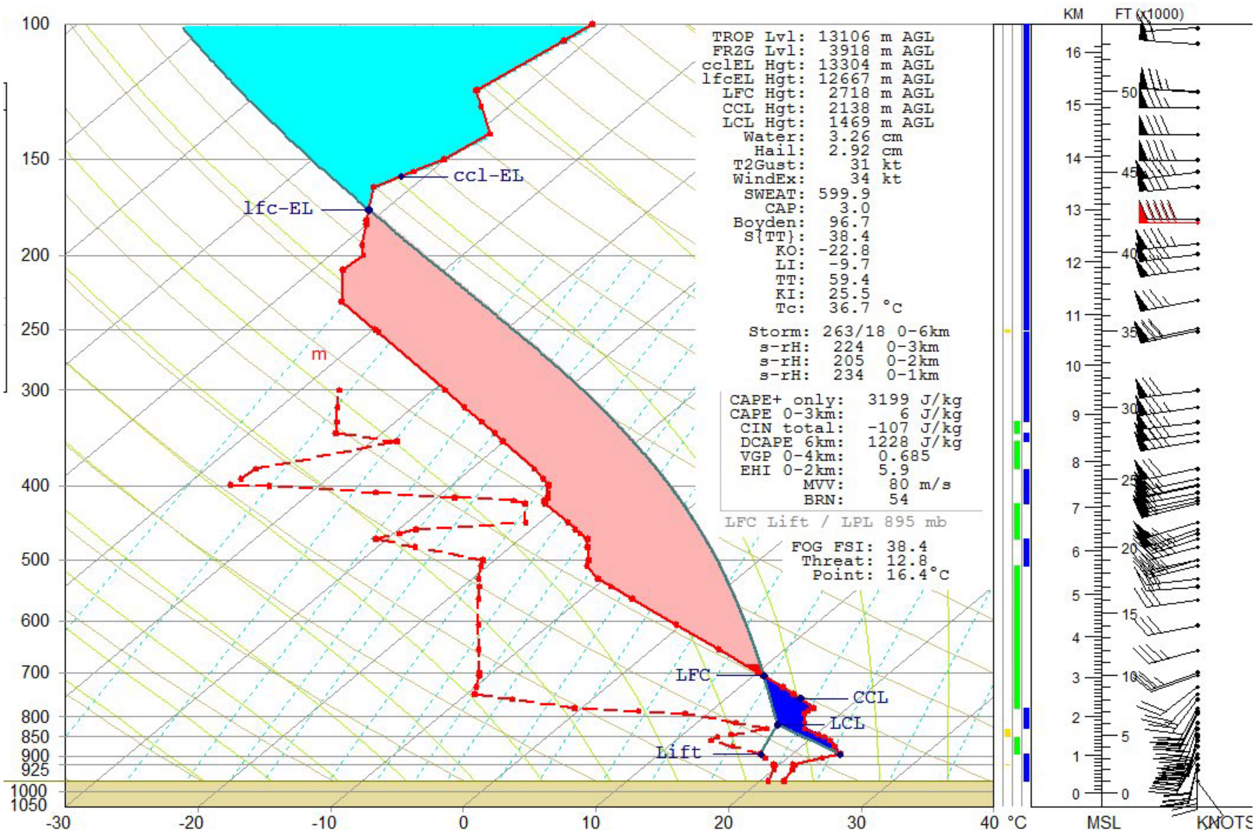

## 7.4 Kelvin-Helmholtz Instability

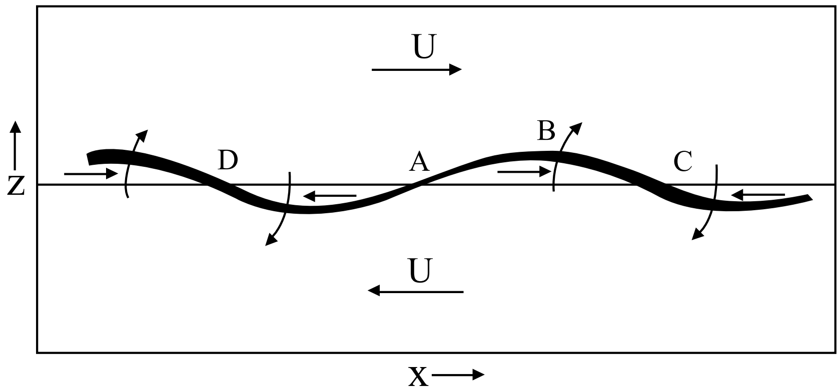


Fig. 7.8: A sketch illustrates the growth of a sinusoidal disturbance to an initially uniform vortex sheet (dashed) with positive vorticity normal to the paper. The local strength of the vortex sheet is represented by the thickness of the sheet. The curved arrows indicate the direction of the self-induced movement of the vorticity in the sheet, and show (a) the accumulation of vorticity at points like *A* and (b) the general rotation about points like *A*, which together lead to exponential growth of the disturbance. (Adapted after Batchelor 1967 and Drazin and Reid 1981)

Fig. 7.9: An example of breaking Kelvin-Helmholtz waves in clouds (billow clouds) formed over Laramie, Wyoming, USA. (Photo by Brooks Martner, NOAA Environmental Technology Laboratory)

- The shear instability occurs in a stratified fluid flow in vertical is called K-H instability. The criterion for the K-H instability to occer is based on Miles' theorem: $Ri < 1/4$ somewhere in the stratified fluid is a necessary condition for instability to occur.

➢ The K-H instability can also be understood by using the energy argument presented below (as characterized by Chandrasekhar 1961). To quantify the effects of buoyancy and vertical shear, we consider two neighboring fluid parcels of equal volumes at heights $z$ and $z+\delta z$ and interchange them. The work $\delta W$ that must be done to incur this interchange against gravity is given by

$$\Delta W = -g\,\delta\bar{\rho}\,\delta z\,, \qquad (7.4.1)$$

where $\delta\bar{\rho}=(d\bar{\rho}/dz)\delta z$ is the difference in the basic density at the two heights. The kinetic energy per unit volume available to do this work is given by

$$\Delta K = \left\{\underset{1}{\frac{1}{2}\rho U^2} + \underset{2}{\frac{1}{2}\rho(U+\delta U)^2}\right\} - \underset{3}{\frac{\rho}{2}\frac{[U+(U+\delta U)]^2}{2}} = \frac{1}{4}\bar{\rho}(\delta U)^2\,. \qquad (7.4.2)$$

In (7.4.2), terms 1 and 2 respectively represent the kinetic energies of air parcels 1 and 2 before the interchange, while term 3 represents the kinetic energy of the air parcels after the interchange. A necessary condition for this interchange, and thus for instability, is that $\Delta W \le \Delta K$ somewhere in the flow:

$$Ri \equiv \frac{N^2}{U_z^2} = \frac{-(g/\bar{\rho})\,d\bar{\rho}/dz}{(dU/dz)^2} < \frac{1}{4}\,. \qquad (7.4.3)$$

## 7.5 Inertial Instability

- For typical atmospheric conditions $N^2 > 0$ , the vertically displaced air parcel either returns to its original position or acts to stabilize vertical displacement.
- Analogous to the static instability, rotation tends to return the horizontally displaced air parcel to its original position or stabilize the displacement.
- This is similar to how buoyancy tends to return or stabilize the vertically displaced air parcel. This type of instability is called *inertial instability*.
- We have *inertial instability* if the horizontally displaced parcel accelerates away from its original position.

[ref] The equations of motion for an inviscid, Boussinesq fluid in the cylindrical polar coordinates $(r, \theta, z)$ may be written as

$$\frac{Du}{Dt} - \frac{V^2}{r} = -\frac{1}{\rho_o}\frac{\partial p}{\partial r}, \tag{7.5.1}$$

$$\frac{DV}{Dt} + \frac{uV}{r} = -\frac{1}{\rho_o r}\frac{\partial p}{\partial \theta}, \tag{7.5.2}$$

$$\frac{Dw}{Dt} = -\frac{1}{\rho}\frac{\partial p}{\partial z}, \tag{7.5.3}$$

where $r$ is the radius or distance from the axis of rotation, $(u, V, w)$ are the radial, azimuthal (tangential) and vertical velocities, respectively, and the total derivative is defined as $D/Dt \equiv \partial/\partial t + u\,\partial/\partial r + w\,\partial/\partial z$.
The equation of mass conservation is

$$\frac{\partial u}{\partial r} + \frac{u}{r} + \frac{\partial w}{\partial z} = 0. \tag{7.5.4}$$

Since the tangential velocity is related to *angular momentum* per unit mass (*M*) and angular velocity $(\Omega)$ by $M \equiv Vr = \Omega r^2$, Eq. (7.5.2) can be rewritten as

$$\frac{DM}{Dt} = \frac{D(Vr)}{Dt} = 0, \tag{7.5.5}$$

Thus the angular momentum is conserved for an axisymmetric motion in an inviscid fluid. Note that the circumference around the circle of radius $r$ is $2\pi M$ .

The mean state is assumed to have no radial acceleration. In other words, it is said to be in *cyclostrophic flow* balance (e.g. see Holton 2004), meaning that the pressure gradient force in the environment is balanced by the centrifugal force

$$-\frac{\overline{M}^2}{r^3} = -\frac{\overline{V}^2}{r} = -\frac{1}{\rho_o}\frac{\partial \overline{p}}{\partial r}. \quad (7.5.6)$$

According to parcel theory, the motion does not perturb the pressure field of the environment. It is from this theory that we make our assumptions.

Thus, (7.5.1) becomes

$$\frac{Du}{Dt} = -\frac{1}{\rho_o}\frac{\partial p}{\partial r} + \frac{\overline{V}^2}{r} = \frac{1}{r^3}\left(M^2 - \overline{M}^2\right). \qquad (7.5.7)$$

To illustrate the concept of inertial stability, let us consider that the square of environmental angular momentum ($\overline{M}^2$) increases with the radius and the vortex circular motion is assumed to be in *solid body rotation*, as shown in Fig. 7.10.

Fig. 7.10: Schematic representation of an inertially stable system of fluid confined by a rotating cylinder. The square of environmental angular momentum ( $\overline{M} \equiv u_\theta r = \Omega r$ ) is assumed to increase with radius. (Adapted after Emanuel 1994)

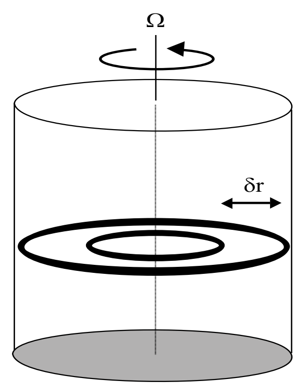


- Now consider a ring of fluid displaced radially outward.
- The conservation of angular momentum ( $M \equiv Vr = \Omega r^2$ ) provides less angular velocity ( $\Omega$ ) and centrifugal force for the tube than that which is required to balance the local pressure gradient force in the new position. This forces the air tube to accelerate back toward its original position, creating an inertially stable system.

- It can be derived,

$$\frac{Du}{Dt} = -\frac{1}{r_o^3}\frac{\partial \overline{M}^2}{\partial r}\delta r \qquad (7.5.8)$$

at $r_o + \delta r$. Note that *u* is the radial velocity defined as positive outward from the center of rotation.

- Therefore, the fluid motion is *stable* if $\overline{M}^2$ increases with the radius from the axis of rotation.

- This leads to the Rayleigh (1916) criteria for inertial stability, neutrality, and instability for a homogeneous, incompressible and inviscid circular vortex motion

$$\frac{\partial \overline{M}^2}{\partial r} \begin{cases} > 0 & \text{inertially stable} \\ = 0 & \text{inertially neutal} \\ < 0 & \text{inertially unstable} \end{cases} \qquad (7.5.9)$$

- The inertial instability is also called centrifugal instability.
- It can be shown that a *Rankine vortex*, where $V = ar$ for $r \le r_c$ and $V = b/r$ for $r > r_c$, and *a* and *b* are constants, is inertially stable for $r \le r_c$ and neutral for $r > r_c$.

- Note that a Rankine vortex is often used to represent the circulation of a tornado vortex core or a tropical cyclone in numerical modeling simulations, as in the so-called *bogusing* technique.

- The criterion for inertial instability for $u_g$ can be derived by considering

$$\frac{Du}{Dt} = f(v - v_g) = f(M - \overline{M}), \qquad (7.5.1)$$

$$\frac{Dv}{Dt} = -fu - \frac{1}{\rho}\frac{\partial p}{\partial y} = -fu = -f\frac{Dx}{Dt}. \qquad (7.5.2)$$

where $M = v + fx$ is the absolute momentum and $\overline{M} = v_g + fx$ is the geostrophic absolute momentum of the basic state of the fluid.

Now consider a parcel whose initial location is at $x = x_o$ and moves with the basic flow. If the air parcel is displaced a small distance ($\delta x$) to $x = x_o + \delta x$, the new meridional velocity can be obtained by integrating (7.5.2),

$$v(x_o + \delta x) = v_g(x_o) - f\,\delta x. \qquad (7.5.3)$$

The geostrophic wind at the new location can be approximated by

$$v_g(x_o + \delta x) = v_g(x_o) + \frac{\partial v_g}{\partial x}\delta x. \qquad (7.5.4)$$

Substituting (7.5.3) and (7.5.4) into (7.5.1) at $x_o + \delta x$ leads to,

$$\frac{D^2 \delta x}{Dt^2} + f\left(\frac{\partial v_g}{\partial x} + f\right)\delta x = 0, \qquad (7.5.5)$$

Thus, the criteria for inertial stability, neutrality, and instability are:

$$f\frac{\partial \bar{M}}{\partial x} = f\left(\frac{\partial v_g}{\partial x} + f\right) \begin{cases} > 0 & \text{inertially stable} \\ = 0 & \text{inertially neutral} \\ < 0 & \text{inertially unstable} \end{cases} \quad (7.5.6)$$

- Similarly for an air parcel that is moving with the geostrophic basic state motion at a position $y = y_o$,

$$u(y_o + \delta y) = u_g(y_o) + f\delta y\,,$$

it can be derived

$$\frac{D^2 \delta y}{Dt^2} = -f(f - \frac{\partial u_g}{\partial y})\delta y = -\frac{\partial M}{\partial y}\delta y$$

where $M \equiv -f(f - \partial u_g / \partial y)$ is the absolute momentum. The criteria for inertial stability, neutrality, and instability are:

$$f\frac{\partial \bar{M}}{\partial y} = f\left(f - \frac{\partial u_g}{\partial y}\right) \begin{matrix} > 0 & \text{inertially stable} \\ = 0 & \text{inertially neutral} \\ < 0 & \text{inertially unstable} \end{matrix} \quad (7.5.7)$$

- Based on (7.5.7), the inertial instability can be illustrated by

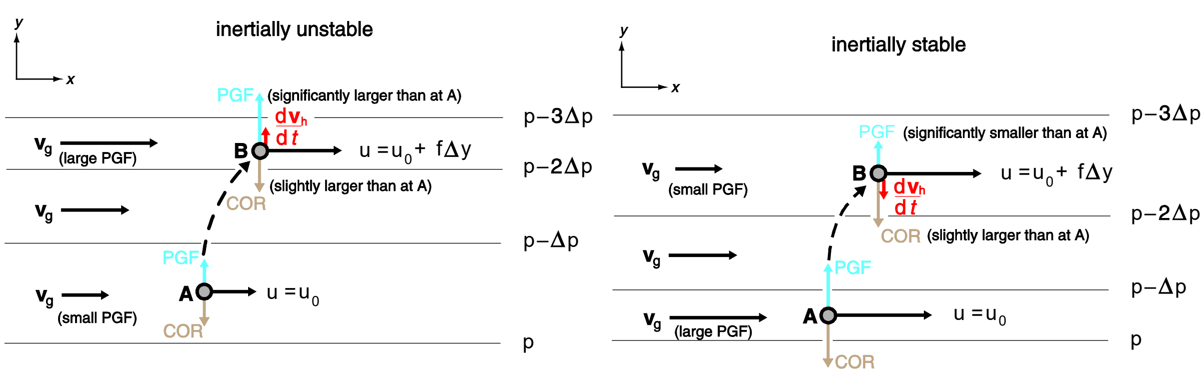


(Markowski and Richardson, 2010; curtesy of Dr. Markowski)

## 7.6 Symmetric Instability

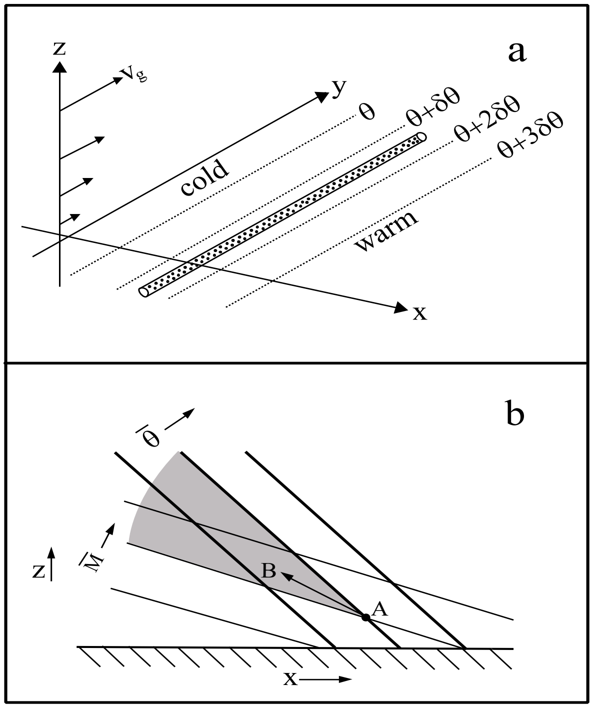


Fig. 7.11: A schematic of a mean state with symmetric instability. (a) A meridional, steady baroclinic flow. The unidirectional geostrophic wind $v_g$ is in thermal wind balance. One may imagine an idealized broad front is aligned with y-axis and located in between the cold and warm region. Under this situation, $v_g$ is the along-front wind. (b) The $\bar{M}$ and $\bar{\theta}$ surfaces on the $x$-$z$ plane are tilted such that both of them increase upward and eastward. Displacement of an air parcel upward anywhere within the shaded area from point A is symmetrically unstable (Adapted after Houze 1993).

- As discussed in previous sections, if a dry or unsaturated atmosphere satisfies the criteria for static (gravitational) stability ( $N^2 > 0$ ) and inertial stability ( $f\,\partial\bar{M}/\partial x = f\,(\partial v_g/\partial x + f) > 0$; $\bar{M} = v_g + fx$ is the angular momentum) separately, then an air parcel displaced either vertically or horizontally in the atmosphere will return to its original position.

- However, under certain conditions, it is possible for an air parcel to accelerate away from its original position if it is displaced along a slantwise path.

- This type of instability is called *symmetric instability*, and is called so because the basic state and perturbations are independent of the horizontal coordinates. Due to this reason, both $\partial/\partial x = 0$ and $\partial/\partial y = 0$ have been used to refer to this state in the literature. In the previous section, we assumed $\partial/\partial y = 0$ and thus defined $M = v + fx$.

- On the other hand, if we assume $\partial/\partial x = 0$, then the absolute momentum may be defined as $M = u - fy$ and the inertial instability criterion becomes $-f\,\partial\overline{M}/\partial y = f\,(f - \partial u_g/\partial y) < 0$. Symmetric instability has also been referred to as *isentropic inertial instability* in the literature.

- In a dynamic sense, static, potential, inertial, and symmetric instabilities are very closely related. Each of the instabilities can be thought of as resulting from an unstable distribution of body forces acting on a fluid element.

  The responsible body forces are the gravitational force for static and potential instabilities, centrifugal force for inertial instability, and a combination of gravitational forces in the vertical and centrifugal forces in the horizontal for symmetric instability.

  Due to the combination of these two forces, symmetric instability occurs when the motion is slantwise.

### *7.6.1 Dry Symmetric Instability*

- The symmetric instability in a dry atmosphere can be understood by applying the parcel argument. For convenience, consider a Boussinesq fluid in which the basic flow and disturbances are independent of the *y* direction, i.e. $\partial/\partial y = 0$, as was assumed earlier in the derivation of criterion for inertial instability. The air parcel can now be viewed as a tube of air extending infinitely along the *y*-axis.

- To demonstrate that symmetric instability may occur when the basic flow is both statically and inertially stable, we consider the mean state of the atmosphere as illustrated in Fig. 7.11.

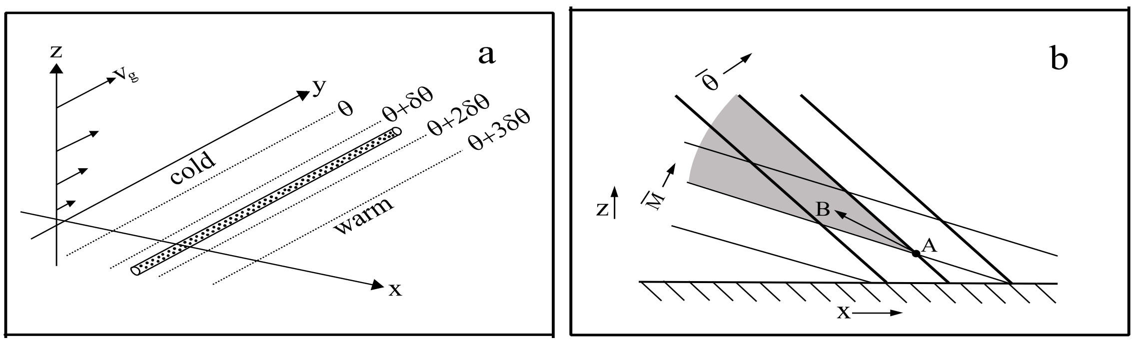


- The basic flow is also assumed to be in hydrostatic and geostrophic balance, i.e. in thermal wind balance,

$$f\frac{\partial v_g}{\partial z} = \frac{g}{\theta_o}\frac{\partial \overline{\theta}}{\partial x}, \qquad (7.6.1)$$

where $\overline{\theta}(x)$ and $\theta_o$ are the mean potential temperature and a constant reference potential temperature, respectively.

- Imagine that an idealized front is aligned with the *y*-axis and located between the cold and warm regions as sketched in Fig. 7.11a.

Under this situation, $v_g$ becomes the along-front wind. The $\overline{M}$ and $\overline{\theta}$ surfaces on the *x-z* plane are tilted such that both $\overline{\theta}$ and $\overline{M}$ increase upward and eastward (Fig. 7.11b).

Since $\partial\overline{\theta}/\partial z > 0$, an air parcel displaced upward (downward) from A will have a lower (higher) value of $\overline{\theta}$ than its environment, assuming no perturbation of the environment by the parcel and immediate adjustment of the parcel's pressure to that of its environment. Thus, the parcel density is greater (smaller) than the environment for upward (downward) motion and results in negative buoyancy, which forces the parcel to accelerate back to its origin.

Analogously, since $\partial \overline{M} / \partial x > 0$, an air parcel displaced horizontally in the negative direction from point $A$ in Fig. 7.11 acquires a positive value of ( $M - \overline{M}$ ) and is accelerated back toward A, according to Eq. (7.5.10).

- Displacement of an air parcel along a $\overline{M}$ surface, as shown in Fig. 7.11, will not cause the parcel to experience any horizontal acceleration since its $M$ value is conserved in the displacement.

  Similarly, a parcel displaced along the $\bar{\theta}$ surface will not experience any vertical acceleration.

  However, displacement of an air parcel upward anywhere within the shaded wedge, will subject the parcel to an upward and leftward acceleration in the direction of its initial displacement since $\bar{\theta}$ decreases and $\overline{M}$ increases along the displacement AB. This is called *symmetric instability* or more specifically *dry symmetric instability*.

- Dry symmetric instability can also be viewed as either dry static (gravitational) instability on a $\overline{M}$ surface, i.e. $\partial \bar{\theta} / \partial z|_{M_g} < 0$, or inertial instability on an isentropic surface, i.e. $\partial \overline{M} / \partial x|_{\bar{\theta}} < 0$. Thus, any slantwise displacement within the wedge expanded between $\overline{M}$ and $\bar{\theta}$ may release the symmetric instability.

- The occurrence of symmetric instability requires

$$-\left.\frac{\partial z}{\partial x}\right|_{\bar{\theta}} > -\left.\frac{\partial z}{\partial x}\right|_{\bar{M}} . \qquad (7.6.2)$$

Based on coordinate transformation (e.g. Holton 2004), we have

$$\left.\frac{\partial z}{\partial x}\right|_{\bar{\theta}} = -\frac{\partial\bar{\theta}/\partial x}{\partial\bar{\theta}/\partial z}; \qquad \left.\frac{\partial z}{\partial x}\right|_{\bar{M}} = -\frac{\partial\bar{M}/\partial x}{\partial\bar{M}/\partial z} . \qquad (7.6.3)$$

Substituting (7.6.3) into (7.6.2) leads to

$$\frac{(\partial\bar{\theta}/\partial x)(\partial\bar{M}/\partial z)}{(\partial\bar{\theta}/\partial z)(\partial\bar{M}/\partial x)} > 1 . \qquad (7.6.4)$$

- The necessary condition for the dry symmetric instability

$$\frac{R_i}{f}\left(\frac{\partial v_g}{\partial x} + f\right) < 1 \text{, or} \qquad (7.6.5a)$$

$$R_i < \frac{f}{\zeta_{ga}} , \qquad (7.6.5b)$$

where $R_i = N^2/(\partial v_g/\partial z)^2$ is the Richardson number and $\zeta_{ga}$ is the geostrophic absolute vorticity.

- We find that symmetric instability is favored by low static stability, strong basic state wind shear, and anticyclonic relative vorticity. If there no horizontal wind shear exists, the above criterion is reduced to $R_i < 1$ .

**Table 7.1:** Conditions for different types of instabilities (Lin 2007)

| | Static (Gravitational) | Inertial | Symmetric |
|---|---|---|---|
| Dry | Absolute Instability | Inertial Instability | Symmetric Instability |
| | $\partial\bar{\theta}/\partial z < 0$; $\gamma > \Gamma_d$ | $\partial\bar{M}/\partial x < 0$; $\zeta_{ga} + f < 0$ | $(\partial\bar{\theta}/\partial z)_{\bar{M}} < 0$; $(\partial\bar{M}/\partial x)_{\bar{\theta}} < 0$ $\Gamma_d\vert_{\bar{M}} < \gamma\vert_{\bar{M}}$ $\vert\partial z/\partial x\vert_{\bar{M}} < \vert\partial z/\partial x\vert_{\bar{\theta}}$ $PV_g < 0$ |
| Moist | Moist Absolute Instability | N/A | N/A |
| | $\Gamma_s < \gamma_s$ | | |
| Conditional[#] | Conditional Instability (CI) | N/A | Conditional Symmetric Instability (CSI) |
| | $\partial\bar{\theta}_e^*/\partial z < 0$ $\Gamma_s < \gamma < \Gamma_d$ (parcel lifted above LFC) | | $\partial\bar{\theta}_e^*/\partial z\vert_{\bar{M}} < 0$; $\partial\bar{M}/\partial z\vert_{\bar{\theta}_e^*} < 0$ $\Gamma_s\vert_{\bar{M}} < \gamma\vert_{\bar{M}} < \Gamma_d\vert_{\bar{M}}$ $\vert\partial z/\partial x\vert_{\bar{M}} < \vert\partial z/\partial x\vert_{\bar{\theta}_e^*}$ $MPV_g^* < 0$ (parcel lifted above LFC) |
| Potential[##] | Potential Instability (PI) | N/A | Potential Symmetric Instability (PSI) |
| | $\partial\bar{\theta}_e/\partial z < 0$ | | $\partial\bar{\theta}_e/\partial z\vert_{\bar{M}} < 0$; $\partial\bar{M}/\partial z\vert_{\bar{\theta}_e} < 0$ $\vert\partial z/\partial x\vert_{\bar{M}} < \vert\partial z/\partial x\vert_{\bar{\theta}_e}$ $MPV_g < 0$ |

[#]at saturation, $\bar{\theta}_e = \bar{\theta}_e^*$; ## $\bar{\theta}_w$ can be used equivalently for $\bar{\theta}_e$. Meanings of the symbols: (1) $\gamma$: observed environmental lapse rate; (2) $\Gamma_d$: dry lapse rate; (3) $\Gamma_s$: moist lapse rate; (4) $\gamma_s$: observed environmental saturated lapse rate; (5) $\bar{\theta}$: environmental potential temperature; (6) $\bar{\theta}_e$: environmental equivalent potential temperature; (7) $\bar{\theta}_e^*$: environmental saturation equivalent potential temperature; (8) $\bar{M}$: environmental geostrophic absolute momentum; (9) $PV_g$: geostrophic potential vorticity (PV); (10) $MPV_g$: geostrophic PV; and (11) $MPV_g^*$: saturated geostrophic potential vorticity.

### 7.7 Baroclinic Instability (Brief Introduction)

Take Eady's approach (see e.g., Holton 2004), assuming

(i) Basic state density constant (Boussinesq approximation).
(ii) $f$-plane geometry ($\beta = 0$).
(iii) $\partial\overline{u}/\partial z^* = \Lambda =$ constant.
(iv) Rigid lids at $z^* = 0$ and $H$.

The QG potential vorticity equation and thermodynamic energy equation are

$$\left(\frac{\partial}{\partial t} + \overline{u}\frac{\partial}{\partial x}\right)\left(\nabla^2\psi' + \varepsilon\frac{\partial^2\psi'}{\partial z^{*2}}\right) = 0 \qquad (8.62)$$

and

$$\left(\frac{\partial}{\partial t} + \overline{u}\frac{\partial}{\partial x}\right)\frac{\partial\psi'}{\partial z^*} - \frac{\partial\psi'}{\partial x}\frac{\partial\overline{u}}{\partial z^*} + w^*\frac{N^2}{f_0} = 0 \qquad (8.63)$$

respectively, where again $\varepsilon \equiv f_0^2/N^2$.

Applying the normal-mode solution, it can be derived

$$d^2\Psi \Big/ dz^{*^2} - \alpha^2\Psi = 0 \qquad (8.65)$$

where $\alpha^2 = \left(k^2 + l^2\right)/\varepsilon$. A similar substitution into (8.63) yields the boundary conditions

$$\left(\Lambda z^* - c\right) d\Psi/dz^* - \Psi\Lambda = 0, \quad \text{at } z^* = 0, H \qquad (8.66)$$

The above leads to

$$\left[\frac{\alpha_c H}{2} - \tanh\left(\frac{\alpha_c H}{2}\right)\right]\left[\frac{\alpha_c H}{2} - \coth\left(\frac{\alpha_c H}{2}\right)\right] = 0 \qquad (8.70)$$

and the baroclinic instability occurs when $\alpha < \alpha_c$ where is defined by

$$\alpha_c H/2 = \coth(\alpha_c H/2)$$

## 7.8 Barotropic Instability (Brief Introduction)

With horizontal shear and b effect included, the linearized form of the quasi-geostrophic vorticity equation (e.g., Holton's (6.18)) can be derived

$$\left(\frac{\partial}{\partial t}+U\frac{\partial}{\partial x}\right)\nabla^2\psi'+\left(\beta-U_{yy}\right)\frac{\partial\psi'}{\partial x}=0 \qquad (7.8.1)$$

where $u'=-\partial\psi'/\partial y$, $v'=\partial\psi'/\partial x$, and $\zeta'=\nabla^2\psi'$.

The term inside the bracket of the second term of (7.8.1) can be rewritten as

$$\beta-U_{yy}=\frac{d}{dy}\left(f-U_y\right)=\frac{d}{dy}\left(f+\zeta_o\right). \qquad (7.8.2)$$

Substituting (7.8.2) into (7.8.1) and assuming a normal-mode solution: $\psi'=A(y)\exp(ik(x-ct))$ leads to

$$\frac{d^2A}{dy^2}+\left(\frac{\beta-U_{yy}}{U(y)-c}-k^2\right)A=0. \qquad (7.8.3)$$

After some manipulation, it can be shown the necessary condition for barotropic instability is

$\beta-U_{yy}$ must change sign at certain latitude ($y$=$y_c$).